| | JPY | 04216 | B | Dispatch: 7.4.05 | Journal: JPY | CE: Blackwell |
|---|---|---|---|---|---|---|
| | Journal Name | Manuscript No. | | Author Received: | No. of pages: 16 | PE: Chris/Suma |

*J. Phycol.* ***–*** (2005)

DOI: 10.1111/j.1529-8817.2005.00083.x

# MOLECULAR AND MORPHOMETRIC DATA PINPOINT SPECIES BOUNDARIES IN *HALIMEDA* SECTION *RHIPSALIS* (BRYOPSIDALES, CHLOROPHYTA)[1]

*Heroen Verbruggen,*[2] *Olivier De Clerck*

Phycology Research Group and Center for Molecular Phylogenetics and Evolution, Ghent University, Krijgslaan 281 (S8), B-9000 Gent, Belgium

*Wiebe H. C. F. Kooistra*

Stazione Zoologica "Anton Dohrn," Villa Comunale, 80121 Naples, Italy

*and*

*Eric Coppejans*

Phycology Research Group, Ghent University, Krijgslaan 281 (S8), B-9000 Gent, Belgium

**Molecular systematic studies have changed the face of algal taxonomy. Particularly at the species level, molecular phylogenetic research has revealed the inaccuracy of morphology-based taxonomy: Cryptic and pseudo-cryptic species were shown to exist within many morphologically conceived species. This study focused on section *Rhipsalis* of the green algal genus *Halimeda*. This section was known to contain cryptic diversity and to comprise species with overlapping morphological boundaries. In the present study, species diversity within the section and identity of individual specimens were assessed using ITS1–5.8S–ITS2 (nrDNA) and *rps*3 (cpDNA) sequence data. The sequences grouped in a number of clear-cut genotypic clusters that were considered species. The same specimens were subjected to morphometric analysis of external morphological and anatomical structures. Morphological differences between the genotypic cluster species were assessed using discriminant analyses. It was shown that significant morphological differences exist between genetically delineated species and that allocation of specimens to species on the basis of morphometric variables is nearly perfect. Anatomical characters yielded better results than external morphological characters. Two approaches were offered to allow future morphological identifications: a probabilistic approach based on classification functions of discriminant analyses and the classical approach of an identification key.**

***Key index words:*** **anatomy; discriminant analysis; DNA bar coding; genotypic cluster species; *Halimeda incrassata*; *Halimeda melanesica*; morphology; morphometrics; species delineation; taxonomy**

***Abbreviations:*** **DA, discriminant analysis; ITS, internal transcribed spacer; MP, maximum parsimony; PCA, principal component analysis**

The last two decades have seen the incorporation of molecular phylogenetic methods in algal systematic research. Several studies have shown that morphological taxonomic insights did not correspond with the evolutionary history inferred from DNA sequences. This has been especially true for species-level studies, in which many cases of cryptic and pseudo-cryptic diversity were revealed (van der Strate et al. 2002, Gurgel et al. 2003, Zuccarello and West 2003, Cohen et al. 2004). Cryptic species are species that are morphologically indistinguishable, whereas pseudo-cryptic entities are distinguishable morphologically once the appropriate characters are considered (Knowlton 1993). Such key traits may not immediately catch the attention of the observer because they are often more subtle than trends in environmentally induced phenotypic plasticity shared among the entities. Morphological plasticity in its own right has also led to erroneous taxonomy; several molecular phylogenetic studies have demonstrated that morphological oddities at the fringes of the plasticity spectrum have been described as new species (Zuccarello and West 2002, Yano et al. 2004, Kooistra and Verbruggen 2005).

Thalli of the tropical green algal genus *Halimeda* are composed of green calcified segments (Lamouroux 1812, Hillis-Colinvaux 1980). Anatomically, the thalli consist of a single, branched, siphonous cell. The highly organized siphonous branches form the segments and string them together (Barton 1901, Hillis-Colinvaux 1980). *Halimeda* is a well-studied example of a genus in which species diversity was underestimated by morphology-based taxonomy. First, all but

[1]Received 23 November 2004. Accepted 13 February 2005.
[2]Author for correspondence: e-mail heroen.verbruggen@ugent.be.

one of the pantropical species were shown to consist of two unrelated species, one inhabiting the Caribbean and a second populating Indo-Pacific coasts (Kooistra et al. 2002). Second, a considerable number of additional cryptic species were found within both ocean basins (Verbruggen and Kooistra 2004, Verbruggen et al. submitted).

Systematists are now facing the challenge of distinguishing among species that have not been recognized by many generations of alpha-taxonomists. In an attempt to provide a tool for this purpose, Verbruggen et al. (2005a,b) applied a series of morphometric techniques to nine *Halimeda* species representing the five sections of the genus. The present study puts the morphometric techniques explored in Verbruggen et al. (2005a) into practice within *Halimeda* section *Rhipsalis*. In this section, medullar siphons that go through the nodes between segments fuse with their neighbors laterally, resulting in a meshwork of pores interconnecting the siphons at the height of the node (Kooistra et al. 2002, Verbruggen and Kooistra 2004). The section is further characterized by segment agglutination in the basal thallus region (Kooistra et al. 2002, Verbruggen and Kooistra 2004). Most species belonging to section *Rhipsalis* grow on sandy or muddy substrates of tropical lagoons and mangroves. Their holdfast is modified into a large bulbous structure to allow attachment in loose substratum. However, this holdfast type is not a defining trait for the section because bulbous holdfasts can be found, at times, in other sections (Verbruggen and Kooistra 2004) and one species in the section (*H. melanesica*, species authorities listed in Appendix 1) has lost the bulbous holdfast secondarily (Kooistra et al. 2002, Verbruggen and Kooistra 2004).

The section features several taxonomic problems. First, Noble (1987) noticed that the absence of nodal fusions, which sets *H. melanesica* apart from other species, was not constant within the species. She noted considerable blurring of the boundary between *H. melanesica* and *H. incrassata* because of this variability. Second, *H. incrassata* turned out to consist of two unrelated species, one in the Atlantic and one in the Indo-Pacific (Kooistra et al. 2002). The morphological boundaries between the entities remained a mystery. Third, current species boundaries contradict genetic patterns in the species pair *H. simulans–borneensis*. On a morphological basis, *H. borneensis* was thought to be restricted to southwest Pacific waters. *Halimeda simulans* was reported from the Caribbean and several locations in the Indo-Pacific (Hillis-Colinvaux 1980). Verbruggen et al. (2005a) showed that Indo-Pacific specimens identified as *H. simulans* did not belong to the clade of Atlantic *H. simulans* but instead clustered with *H. borneensis*. Fifth, a similar situation occurs with the *H. monile–cylindracea* species pair. *Halimeda cylindracea* is an Indo-Pacific species, and Indo-Pacific specimens identified as *H. monile* belong to *H. cylindracea*. Finally, the status of *H. stuposa*, which had never been questioned in traditional taxonomic research, was doubted by Kooistra et al. (2002) because the small subunit sequence obtained from an isotype specimen was nearly identical to that of *H. borneensis*.

This study aims 1) to identify genotypic clusters in a set of internal transcribed spacer (ITS)1–5.8S–ITS2 and *rps*3 sequences and to redefine species on the basis of these clusters, 2) to assess whether it is possible to distinguish between genotypic cluster species on the basis of morphometric variables, 3) to pinpoint species boundaries using morphometric variables, 4) to present a probabilistic approach toward species identification based on measurements of anatomical structures, and 5) to present a more classical identification method (i.e. a dichotomous key).

## MATERIALS AND METHODS

*Specimen collection, DNA sequencing, and phylogenetic inference*. Specimens were collected from natural populations throughout the species' ranges (Appendix 1). Part of the thallus was preserved in ethanol 95% or silica gel for DNA extraction; the remainder of the specimen was preserved in liquid preservative (ethanol 95% or formalin 5%) for morphometric analyses. Specimens were identified using Hillis-Colinvaux (1980).

Extraction of total genomic DNA followed Kooistra et al. (2002), but for a few specimens, a standard cetyl trimethyl ammonium bromide procedure was used. The nuclear ribosomal ITS1–5.8S–ITS2 region and the plastid UCP7 region (*rps*19–*rps*3) were amplified according to Kooistra et al. (2002) and Provan et al. (2004), respectively. Sequences were determined with forward and reverse primers, using an ABI Prism 3100 automated sequencer (Applied Biosystems, Foster City, CA, USA). Of the *rps*19–*rps*3 sequences, partial *rps*19 and the intergenic spacer were discarded, leaving only partial *rps*3 sequences. The *rps*3 sequences were aligned on the basis of their amino acid sequences using ClustalW 1.82 at the EBI (European Bioinformatics Institute) server, with default settings. The ITS1–5.8S–ITS2 sequences were aligned using ClustalW 1.82 (EBI server, default settings). Sequences and alignments were submitted to GenBank (see Appendix 1 for accession numbers) and Treebase (preliminary accession number SN2128).

Both alignments were subjected to maximum parsimony (MP) analysis in PAUP* 4.0b10 (Swofford 2003). Starting trees were obtained by random stepwise addition. A single tree was retained at each step. Branch swapping was achieved by tree bisection-reconnection. Gaps were treated as missing data. The number of rearrangements was limited to 100 million per addition-sequence replicate. The analysis performed 50 addition-sequence replicates and was carried out without outgroup (midpoint rooting). The MP bootstrapping (1000 replicates) was performed using the same MP settings (Felsenstein 1985). Genotypic clusters in the DNA data were identified by eye from the obtained phylograms.

*Morphometrics*. Measurements and morphometric analyses were carried out as detailed in Verbruggen et al. (2005a), with a number of modifications. Per specimen, 10 segments were photographed. These segments were picked at random, after exclusion of apical and noncalcified segments, and segments from the basal thallus zone, as recommended by Verbruggen et al. (2005b). From the aligned digital images, categorical shape variables were scored. Landmarks were placed on the images as described in Figure 2a of Verbruggen et al. (2005a) and served for landmark analysis and calculation of conventional measurements and ratio shape variables. In the light of the conclusions of Verbruggen et al. (2005a), elliptic Fourier analysis of segment outlines

TABLE 1. Variables describing segment morphology.

| | | |
|---|---|---|
| Categorical shape variables | | |
| s01 | form_seg | Categorical segment form: reniform, ovate, elliptical, obovate, cuneate, rectangular |
| s02 | seg_widt | Categorical variable for relative segment width: narrow, medium, broad |
| s03 | stalk | Categorical variable describing the proximal stalk zone: absent, intermediate, present |
| s04 | form_bas | Categorical variable for the form of the segment base: auriculate to acute in five steps |
| s05 | lobedne | Categorical variable describing the segment's lobedness: absent, shallow, medium, deep |
| s06 | numlobes | Number of lobes:1 to 6 (six meaning many) |
| Conventional measurements | | |
| s07 | length | Segment length (mm) |
| s08 | width | Segment width (mm) |
| s09 | attach | Width of attachment zone (mm) |
| s10 | homw | Height of maximal segment width (mm) |
| s11 | thick | Segment thickness (mm) |
| Ratio shape variables | | |
| s12 | thk_len | Relative segment thickness: thickness over length ratio |
| s13 | thk_att | Ratio of segment thickness over the width of the attachment zone |
| Partial warp scores (landmark analysis) | | |
| s14 | pw_UniX | Uniform shape change score X |
| s15 | pw_UniY | Uniform shape change score Y |
| s16 | pw_1X | Partial warp score 1X |
| s17 | pw_1Y | Partial warp score 1Y |
| s18 | pw_2X | Partial warp score 2X |
| s19 | pw_2Y | Partial warp score 2Y |

was omitted. Table 1 lists the segment variables and their abbreviations. Two data sets were constructed from the data: first, one with data of all segments (10 per specimen) and, second, one with a single entry per specimen (median values of segments belonging to the specimen in question).

Measurements of anatomical structures were made according to Verbruggen et al. (2005a), with some slight modifications. Anatomical investigation was limited to a single segment from the central part of the thallus, following the recommendations of Verbruggen et al. (2005b). All anatomical observations were made with an Olympus BX51 microscope (Olympus Europe, Hamburg, Germany). The diameter of side branches of medullar siphons at their constriction was not measured. Peripheral utricles were drawn and digitized as described in Verbruggen et al. (2005a). Images were aligned to have the upper plane of utricles horizontal and were overlain with a pattern of horizontal lines (Fig. 1A). The pattern consisted of five equidistant horizontal lines and was superimposed on the utricle in such a way that the upper line touched the top side of the utricle and the lower line went through the base of the utricle. Ten landmarks (Fig. 1A) were digitized on the pictures using tpsDig 1.40 (Rohlf 2004). From the landmark files, several size and shape variables were calculated (Fig. 1, B and C): utricle height and width, their ratio (formula 1), and the relative width at 75%, 50%, and 25% of the utricle's height (formulas 2, 3, and 4). Table 2 lists the anatomical variables and their abbreviations. Ten replicate measurements per segment were made (e.g. measurements of 10 random peripheral utricles within a single segment). Two data sets were created: first, one with data of all replicates (10 per specimen) and, second, one with a single entry per specimen (median values of replicates). All data sets are available from the corresponding author upon request.

*Statistical analysis of morphometrics*. *Data exploration:* Exploratory data analysis included visual examination of univariate histograms. Measurement data were log-transformed for analyses requiring so (neperian logarithm; indicated with prefix L_ added to the variable name). Principal component analyses (PCAs) were carried out to explore the multivariate data sets in more detail. All PCAs were carried out in Statistica 6.0 (Statsoft, Tulsa, OK, USA).

*Initial discriminant analyses:* The four data sets were subjected to discriminant analysis (DA) using the General Discriminant Analysis module of Statistica (Statsoft). Genotypic clusters found in the molecular phylogenies were used as a priori groups in DA. Classifications were carried out with equal prior probabilities and without cross-validation. All effects were entered at once.

*DA of degenerate data sets:* After initial DA, further DAs were carried out on partial data sets, with the aim of singling out characters or character combinations that allow good separation between species. Structure coefficients of the canonical roots of previous DAs were used as a guide for further DA: Variables uncorrelated with major canonical roots were omitted. Furthermore, we closed in on specific species groups by including only those species in DA.

## RESULTS

*Sequence data, genotypic clusters, and identifications.* Information on length, base composition, and variability

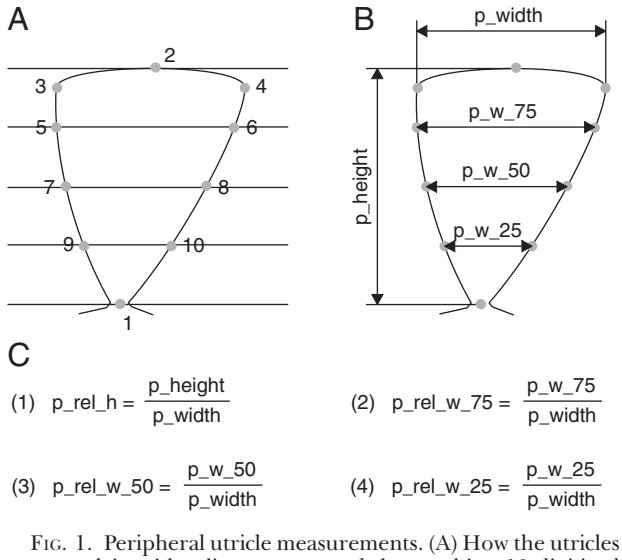


FIG. 1. Peripheral utricle measurements. (A) How the utricles were overlain with a line pattern and the resulting 10 digitized positions. (B) Measurements calculated from the landmark files. (C) Ratios calculated from the measurements.

TABLE 2. Variables describing anatomical structures.

| | | |
|---|---|---|
| Medullar characters | | |
| a01 | diam_ir | Distance between two subsequent ramifications (μm) |
| a02 | constr_m | Medullary siphon diameter (μm) |
| a03 | len_ir | Length over diameter ratio of the siphon segment: len_ir/dia_ir |
| a04 | ir_rel_len | Constriction of main branch diameter (μm) |
| a05 | dichotomy | Fraction dichotomous ramifications |
| a06 | trichotomy | Fraction trichotomous ramifications |
| a07 | quadrichotomy | Fraction quadrichotomous ramifications |
| Nodal properties | | |
| a08 | node_act | Distance from below node to supranodal ramification (μm) |
| a09 | len_supr | Thickness of the supranodal interramification (μm) |
| a10 | diam_supr | Actual pore size or node height (μm) |
| Peripheral utricles | | |
| a11 | p_surf | Surface diameter peripheral utricle (μm) |
| a12 | p_height | Height of peripheral utricle (μm) |
| a13 | p_width | Diameter of peripheral utricle (μm) |
| a14 | p_rel_w_75 | Relative width of peripheral utricle at 3/4 of its height |
| a15 | p_rel_w_50 | Relative width of peripheral utricle at 1/2 of its height |
| a16 | p_rel_w_25 | Relative width of peripheral utricle at 1/4 of its height |
| a17 | p_rel_h | Relative height of utricle: p_height over p_width ratio |
| Secondary utricles | | |
| a18 | s_height | Length (μm) of the secondary utricle |
| a19 | s_width | Maximal diameter (μm) of the secondary utricle |
| a20 | s_rel_h | Relative height of secondary utricle: s_length over s_width ratio |
| a21 | s_succ | Number of peripheral utricles carried by the secondary utricle |
| Tertiary utricles | | |
| a22 | t_height | Length (μm) of the tertiary utricle |
| a23 | t_width | Maximal diameter (μm) of the tertiary utricle |
| a24 | t_rel_h | Relative height of tertiary utricle: t_length over t_width ratio |
| a25 | t_succ | Number of secondary utricles carried by the tertiary utricle |

of sequence data are listed in Table 3. Figures 2 and 3 depict the phylograms obtained by MP analysis of ITS1–5.8S–ITS2 and *rps*3 sequence data, respectively. The trees featured a number of genotypic clusters of closely related specimens separated from other such clusters by long branches with high bootstrap support. Specimens forming a genotypic cluster in the ITS–5.8S–ITS2 tree, also grouped in the *rps*3 tree and vice versa.

Species names were assigned to the genotypic clusters on the basis of correspondence with morphology-based identifications of specimens belonging to the clusters. In a few cases, genotypic clusters and morphological identifications did not match. Several specimens with an *H. simulans* morphology were recovered in the *H. borneensis* cluster, and the *H. incrassata* 1a genotypic cluster contained multiple specimens that stood midway between *H. incrassata* and *H. melanesica* morphologies.

There was a discrepancy in branch lengths between the *H. monile–simulans–incrassata* 2 group and the remainder of the species in the *rps*3 tree, branches between species being much longer within the group in question. Furthermore, within-species sequence divergence was large within *H. monile* and *H. incrassata* 2. These discrepancies were caused by codon indels.

Within the Indo-Pacific *H. incrassata* diversity (named *H. incrassata* 1 in Figs. 2 and 3), two genotypic clusters were present. The first cluster (1a) represented the bulk of the specimens and occurs throughout the Indo-Pacific. The second cluster (1b) contained five specimens from Honolua Bay, Maui, Hawaii. In the ITS1–5.8S–ITS2 tree (Fig. 2), cluster 1b branched off from within cluster 1a, which was left paraphyletic. The branch leading toward cluster b was very long and obtained 100% bootstrap support. In the *rps*3 tree, clusters 1a and 1b were both monophyletic and received high bootstrap support. Cluster 1a was the closest sister to *H. macroloba*; cluster 1b was sister to the *H. macroloba–incrassata* 1a clade. Clusters 1a and 1b were retained as distinct entities for further analyses.

We were unable to obtain *H. stuposa* specimens suitable for DNA analysis. Amplification of DNA from the specimen sequenced by Kooistra et al. (2002) failed on several attempts. As a consequence, this species was not represented in the trees. Nonetheless, *H. stuposa* was retained as a separate entity in further analyses.

*Exploration of morphometric data.* Segment morphological variables were scored from 90 specimens and

TABLE 3. Length, variability, and composition of DNA data.

| | ITS1–5.8S–ITS2 | *rps*3 |
|---|---|---|
| Sequence length | 436–472 | 660–876 |
| Alignment length | 485 | 1014 |
| Constant positions | 338 | 422 |
| Variable positions | 147 | 592 |
| Parsimony informative positions | 116 | 497 |
| T | 19.1% | 26.0% |
| C | 29.3% | 18.7% |
| A | 20.8% | 34.6% |
| G | 30.8% | 20.7% |
| Indels | 5.6% | 26.6% |

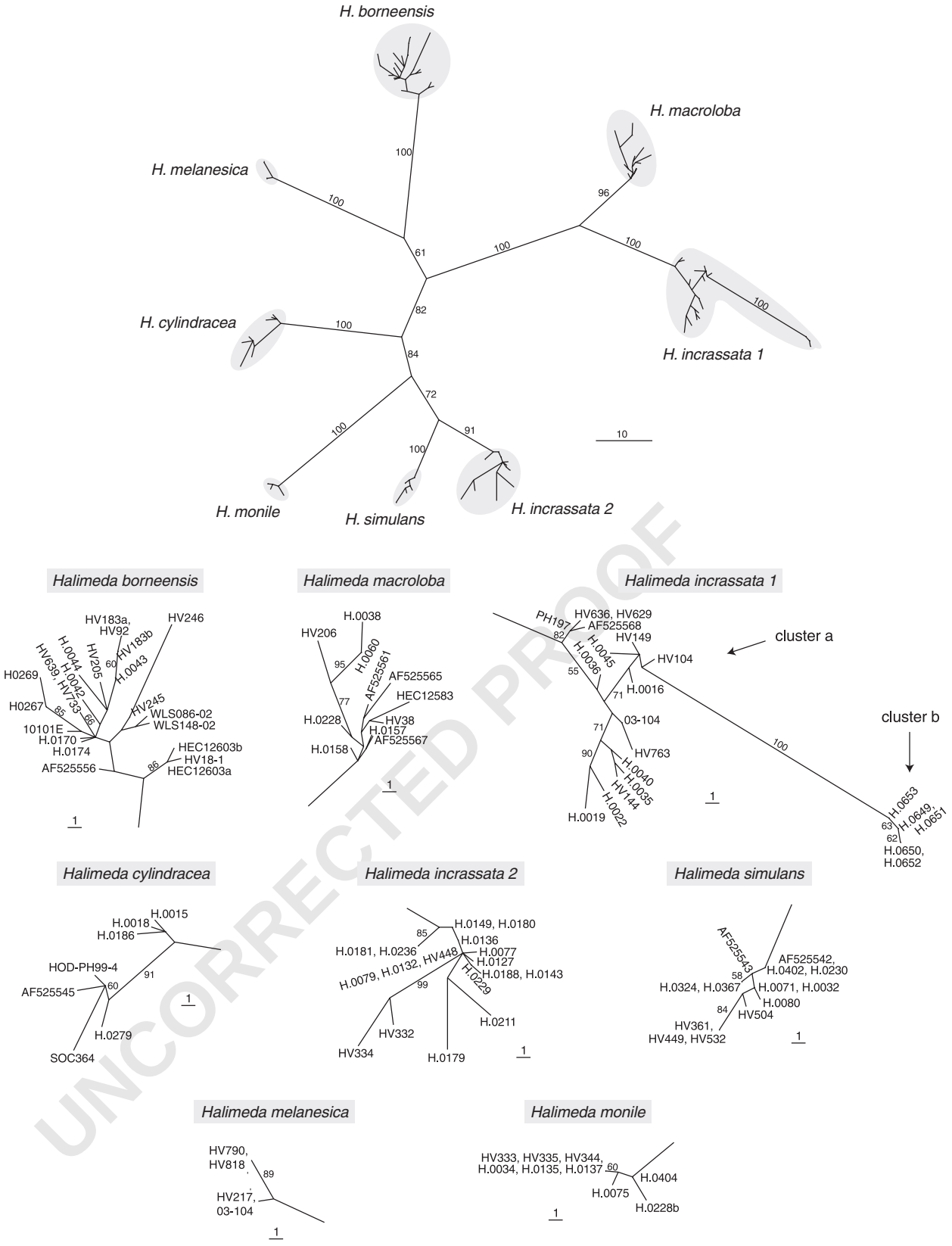




FIG. 2. MP tree inferred from nuclear ribosomal ITS1–5.8S–ITS2 DNA sequences. One of 19 MP trees of 309 steps. MP bootstrap values are indicated at branches.

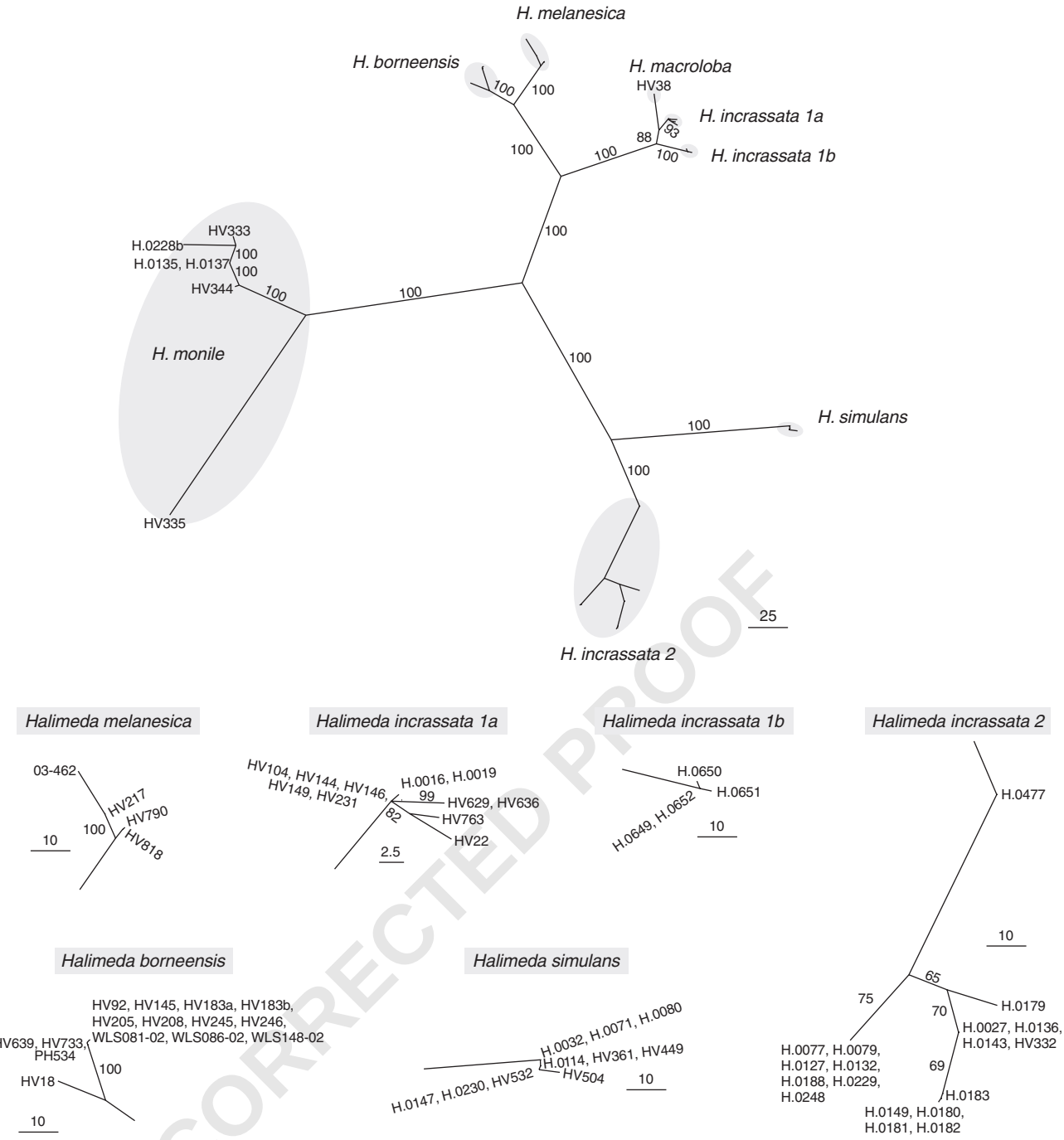


FIG. 3. MP tree inferred from plastid *rps*3 DNA sequences. One of 49 MP trees of 1178 steps. MP bootstrap values are indicated at branches.

anatomical variables from 86 specimens belonging to 10 species (genotypic clusters). This resulted in data for 900 segments, 860 nodal and medullar structures, 860 peripheral utricles, and 1030 secondary and 536 tertiary utricles, adding up to a total of 14,312 anatomical measurements.

Figure 4 shows the biplots of PCA carried out on segment morphological and anatomical data sets (single entry per specimen). In the biplot of segment morphological data (Fig. 4A), certain genotypic clusters occupied nonoverlapping regions (e.g. *H. monile* vs. *H. simulans*, encircled in figure). Most of the genotypic cluster species, however, showed partial or complete overlap in the first two dimensions of principal component space. All species involved in taxonomic problems (see the Introduction) showed mutual overlap except *H. stuposa*, the two specimens of which fell outside of the *H. borneensis* range. Species within the

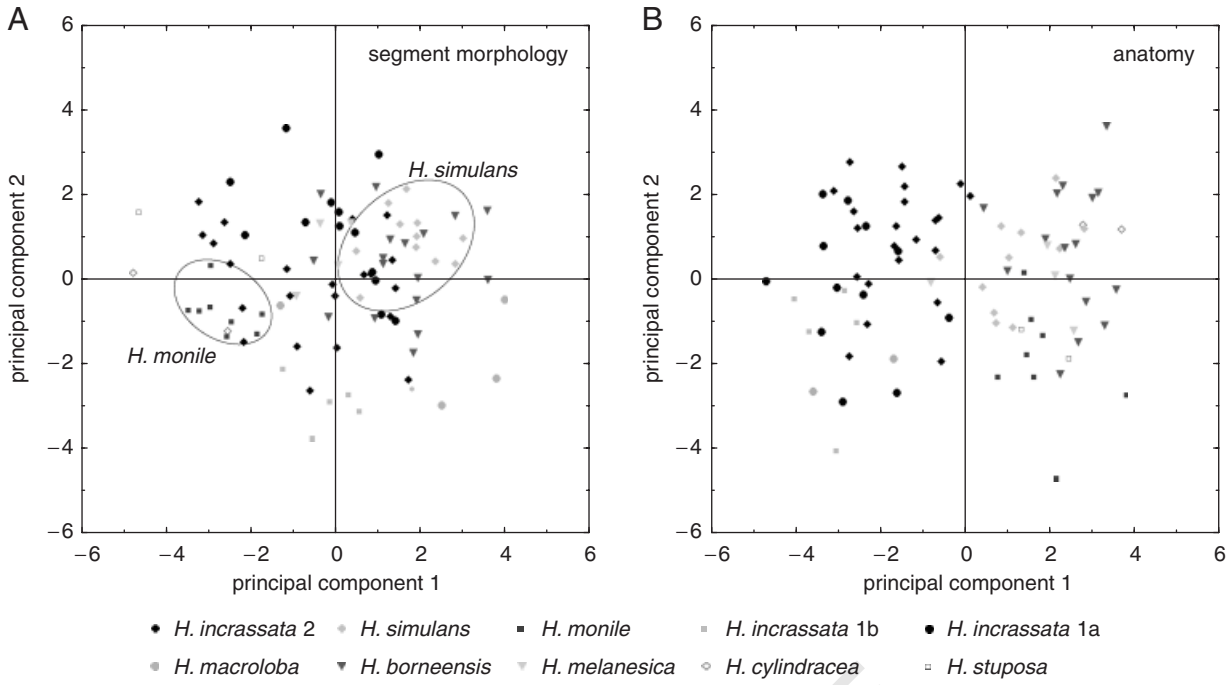


FIG. 4. PCA biplots of segment morphological (A) and anatomical (B) data (one entry per specimen). (A) The areas occupied by *Halimeda monile* and *H. simulans* have been encircled. Variables included in the analysis were the log-transformed s07, s08, s11–s19 for segment morphology and the log-transformed a01–a05, a08–a20, a22–a24 for anatomy.

look-alike species pairs *H. simulans–borneensis* and *H. monile–cylindracea* showed considerable overlap. The three *H. incrassata* genotype cluster species and *H. melanesica* occupied partially overlapping areas.

Principal component analysis of anatomical data resulted in the biplot shown Figure 4B. Genotypic cluster species were far from randomly dispersed on the graph. The left-hand side of the graph (second and third quadrant) contained *H. incrassata* 1a, *H. incrassata* 1b, *H. incrassata* 2, and *H. macroloba*. The first and fourth quadrant (right-hand side of graph) contained the other species. Apart from this basic subdivision, most genotypic cluster species occupied overlapping regions in the biplot.

*Initial DAs.* The DA carried out on the complete sets of medians demonstrated differences between all species. Figure 5 depicts canonical biplots for segment morphological and anatomical data. The biplot of segment morphological data (Fig. 5A) did not show obvious species separation in the first two roots. The anatomical data, on the other hand, separated several species using only the first two canonical roots.

For the segment morphological data, all interspecific distances (squared Mahalanobis distances) were significantly different from zero, except for *H. simulans–borneensis* ($P = 0.2989$), *H. monile–cylindracea* ($P = 0.4036$), and *H. melanesica–incrassata* 1a ($P = 0.2729$). Classification tests based on segment morphology achieved between 58% and 100% success (average 74%), meaning that specimens belonging to a species were allocated to that species in 58% to 100% of the cases tested. The worst classification results were obtained for *H. borneensis*, which was often mistaken for *H. simulans* (4/17). *Halimeda incrassata* 2 was casually misclassified as *H. simulans* (2/23), *H. incrassata* 1a (2/23), or *H. borneensis* (2/23). *Halimeda incrassata* 1a also obtained relatively low classification success. Its specimens were occasionally allocated to various other species. Adding categorical shape variables increased classification success by about 10% (average 83%).

The anatomical data set achieved higher classification success (average 97%). For most species all specimens were correctly classified. Only *H. borneensis* and *H. monile* were mistaken for each other; one specimen was misclassified in each direction. All interspecific squared Mahalanobis distances were significantly different from zero at the 5% significance level.

When the original data (10 replicates per specimen) were used instead of the median values, there was considerably more overlap in the canonical biplots (not shown). Even for the anatomical data, no clear-cut clusters were obvious in the first two canonical dimensions. Nonetheless, classification success was only slightly less; for anatomical data it was rarely lower than 90%.

*Probabilistic identification approach.* Table 4 presents the classification functions of anatomical variables for the 10 studied species. These classification functions resulted from DA of the anatomical data set (median values, excluding tertiary utricles). The functions allowed 96% correct identifications. Misidentifications only occurred for the species *H. monile* and *H. borneensis* (87% correct allocations). All other species obtained 100% classification success.

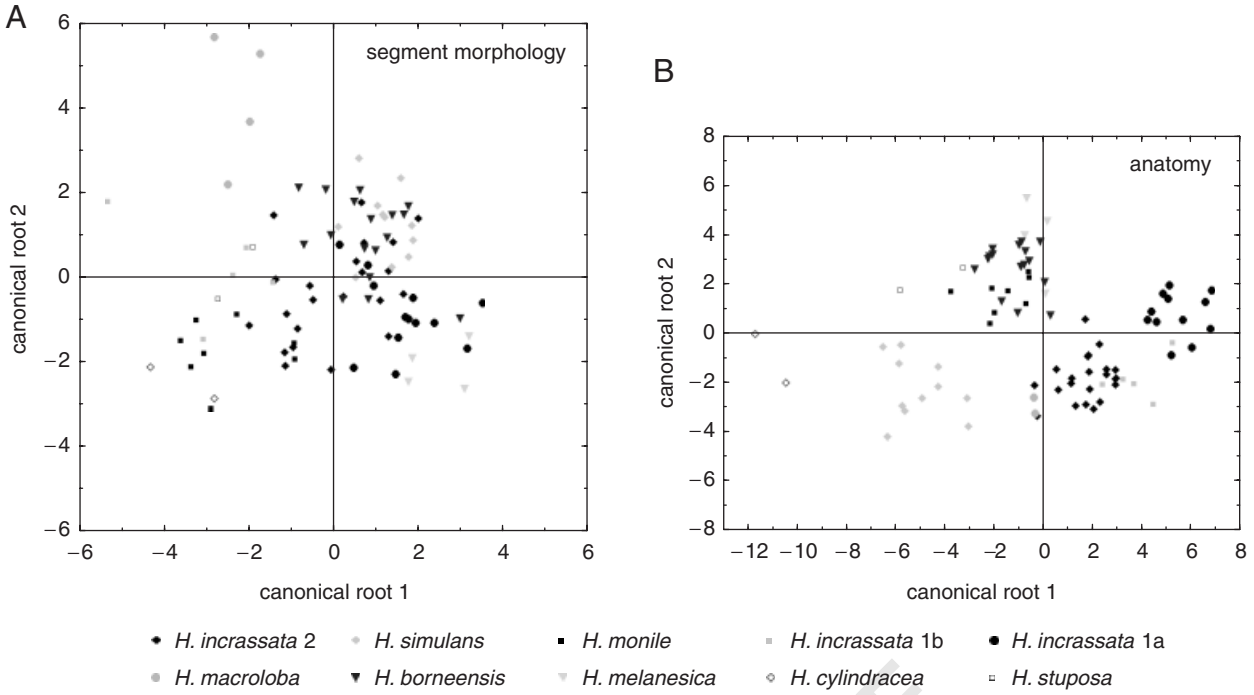


FIG. 5. Discrimination of 10 *Halimeda* species based on segment morphology (A) and anatomy (B). The variables included in DA were s07, s11–s19 for segment morphology and a01–a05, a08–a12, a14–a20, a22–24 for anatomy.

*Additional DAs*. Further DAs, containing only subsets of characters and taxa, were carried out to single out characters with diagnostic value. These results are not presented in full because they are not of general interest. Below, we expand on the distinction between the three *H. incrassata* entities as an example. Instead of reporting the results in full, they were interpreted and used to set up an identification key. This key, presented in Table 5, incorporates traditional and morphometric data and led to 100% correct identifications of the specimens incorporated in this study.

Figure 6A depicts the canonical biplot of the DA carried out on segment morphological data of *H. incrassata* specimens. Entity 1b was distinct; entities 1a and 2 showed considerable overlap. Segment size (represented by L_length) was highly correlated with the principal root and allowed distinction between entity 1b and the other two entities (Fig. 6B). None of the individual segment morphological characters allowed unambiguous distinction between entities 1a and 2. The canonical biplot based on anatomical variables (Fig. 7A) showed perfect separation between all three *H. incrassata* entities. Entities 1a and 2 separated along the first root; entity 1b separated from the rest along the second root. Root 1 had the highest correlation with variables associated with peripheral utricles (L_p_height and L_p_surf). Nonetheless, neither of these characters allowed unambiguous separation between entities 1a and 2 (e.g. L_p_surf: Fig. 7B). The second root showed high correlation with characters associated with nodal anatomy (L_node_act, L_diam_supr and L_len_supr). Length of the supranodal siphon could be used to distinguish between entity 1b and both other entities, but slight overlap of estimated distributions was present between 1a and 1b (Fig. 7C). Because no individual characters could distinguish between entities 1a and 2 unambiguously, combinations of characters were plotted. For example, in the plot of height versus width of peripheral utricles, no overlap was present between the species (Fig. 7D).

## DISCUSSION

*Species delineation and DNA bar coding*. On the basis of DNA sequence data, specimens could be classified into a number of clear-cut genotypic clusters. Whereas within-cluster genetic divergences are comparable among genotypic clusters in the ITS1–5.8S–ITS2 data, the discrepancy in sequence divergences of the *rps*3 data causes within-cluster genetic divergences to be much larger within the *H. monile–simulans–incrassata* 2 clade than those within the remainder of the section. This discrepancy is caused by the presence of codon indels within the *rps*3 gene in the *H. monile–simulans–incrassata* 2 clade. Irrespective of the discrepancy, genotypic clusters are concordant among the markers used.

Now that our set of sequences has been partitioned into clear-cut and named genotypic clusters, identification of new specimens on the basis of DNA bar codes is possible. The use of DNA bar coding as an identification technique is becoming increasingly popular. When using appropriate markers, it allows unambiguous

TABLE 4. Classification functions for anatomical variables.

| Species | Score |
|---|---|
| *Halimeda incrassata* 2 | 81.8 · L_diam_ir − 107.5 · L_constr_m + 146.9 · L_len_ir + 115.9 · L_node_act − 2.13 · L_len_supr + 207.9 · L_diam_supr + 385.8 · L_p_surf + 122.7 · L_p_height + 187.6 L_p_width + 21.9 · L_p_rel_w_75 + 112.5 · L_p_rel_w_50–30.4 · L_p_rel_w_25 + 239.0 · L_p_rel_h − 103.2 · L_s_height + 323.1 · L_s_width − 3028 |
| *H. simulans* | 80.6 · L_diam_ir − 97.1 · L_constr_m + 142.2 · L_len_ir + 113.9 · L_node_act + 0.77 · L_len_supr + 219.9 · L_diam_supr + 333.7 · L_p_surf + 72.0 · L_p_height + 183.5 · L_p_width − 23.5 · L_p_rel_w_75 + 112.4 · L_p_rel_w_50–32.6 · L_p_rel_w_25 + 221.0 · L_p_rel_h − 91.4 · L_s_height + 313.2 · L_s_width − 2697 |
| *H. monile* | 66.8 · L_diam_ir − 102.6 · L_constr_m + 143.9 · L_len_ir + 121.2 · L_node_act + 7.09 · L_len_supr + 212.8 · L_diam_supr + 365.3 · L_p_surf + 89.2 · L_p_height + 203.8 · L_p_width + 2.23 · L_p_rel_w_75 + 107.8 · L_p_rel_w_50–17.6 · L_p_rel_w_25 + 255.9 · L_p_rel_h − 93.5 · L_s_height + 297.6 · L_s_width − 2843 |
| *H. incrassata* 1b | 72.9 · L_diam_ir − 104.4 · L_constr_m + 147.4 · L_len_ir + 123.8 · L_node_act + 4.87 · L_len_supr + 226.4 · L_diam_supr + 401.4 · L_p_surf + 108.0 · L_p_height + 225.6 · L_p_width + 7.46 · L_p_rel_w_75 + 110.9 · L_p_rel_w_50–3.01 · L_p_rel_w_25 + 252.3 · L_p_rel_h − 105.5 · L_s_height + 320.3 · L_s_width − 3279 |
| *H. incrassata* 1a | 62.8 · L_diam_ir − 110.9 · L_constr_m + 151.7 · L_len_ir + 107.0 · L_node_act + 2.47 · L_len_supr + 210.8 · L_diam_supr + 405.5 · L_p_surf + 181.7 · L_p_height + 169.1 · L_p_width + 80.6 · L_p_rel_w_75 + 112.9 · L_p_rel_w_50–46.3 · L_p_rel_w_25 + 224.9 · L_p_rel_h − 106.9 · L_s_height + 313.6 · L_s_width − 3179 |
| *H. macroloba* | 83.2 · L_diam_ir − 108.9 · L_constr_m + 151.8 · L_len_ir + 115.1 · L_node_act + 6.09 · L_len_supr + 213.9 · L_diam_supr + 384.3 · L_p_surf + 128.6 · L_p_height + 146.4 · L_p_width + 24.4 · L_p_rel_w_75 + 147.1 · L_p_rel_w_50–67.6 · L_p_rel_w_25 + 252.9 · L_p_rel_h − 88.0 · L_s_height + 317.6 · L_s_width − 3073 |
| *H. borneensis* | 60.9 · L_diam_ir − 105.9 · L_constr_m + 153.2 · L_len_ir + 109.5 · L_node_act + 2.42 · L_len_supr + 209.8 · L_diam_supr + 369.1 · L_p_surf + 100.2 · L_p_height + 202.8 · L_p_width + 24.2 · L_p_rel_w_75 + 114.1 · L_p_rel_w_50–10.4 · L_p_rel_w_25 + 249.2 · L_p_rel_h − 96.0 · L_s_height + 287.9 · L_s_width − 2777 |
| *H. melanesica* | 54.8 · L_diam_ir − 102.1 · L_constr_m + 140.4 · L_len_ir + 99.3 · L_node_act + 11.24 · L_len_supr + 211.7 · L_diam_supr + 368.8 · L_p_surf + 145.8 · L_p_height + 159.4 · L_p_width − 11.6 · L_p_rel_w_75 + 134.0 · L_p_rel_w_50 − 49.4 · L_p_rel_w_25 + 218.9 · L_p_rel_h − 90.9 · L_s_height + 289.5 · L_s_width − 2769 |
| *H. cylindracea* | 80.6 · L_diam_ir − 84.7 · L_constr_m + 132.8 · L_len_ir + 108.2 · L_node_act + 3.99 · L_len_supr + 222.9 · L_diam_supr + 289.6 · L_p_surf + 70.4 · L_p_height + 136.7 · L_p_width − 35.8 · L_p_rel_w_75 + 114.8 · L_p_rel_w_50 − 34.2 · L_p_rel_w_25 + 184.8 · L_p_rel_h − 77.2 · L_s_height + 302.3 · L_s_width − 2395 |
| *H. stuposa* | 76.8 · L_diam_ir − 104.8 · L_constr_m + 146.7 · L_len_ir + 103.2 · L_node_act − 3.52 · L_len_supr + 218.7 · L_diam_supr + 330.7 · L_p_surf + 91.8 · L_p_height + 174.3 · L_p_width − 95.0 · L_p_rel_w_75 + 140.4 · L_p_rel_w_50 − 54.7 · L_p_rel_w_25 + 251.6 · L_p_rel_h − 76.0 · L_s_height + 289.4 · L_s_width − 2656 |

Specimens can be identified by filling in the values obtained for the different variables. The species that receives the highest score is the species to which the specimen belongs with the highest probability. Probability values can be calculated by dividing the scores for each species by the sum of all scores. *Halimeda favulosa* is not included; this species can be easily recognized by its exceptionally large peripheral utricles (see line 1 of identification key, Table 5).

identification, helps unmask look-alike species regardless of their life stage, and has the potential to reveal the existence of species new to science (Besansky et al. 2003, Hebert et al. 2004a,b, Hogg and Hebert 2004). Our aim, however, was not to replace traditional identification methods by DNA bar coding but rather to have DNA sequence data serve as a foundation on which to construct a new taxonomy, based on reliable morphological differences between species.

*Evolution of* Halimeda incrassata *1*. It is beyond doubt that clusters a and b of *H. incrassata* 1 are distinct from one another. In the *rps*3 tree both are monophyletic. In the ITS1–5.8S–ITS2 tree, *H. incrassata* 1b branches off from within the paraphyletic *H. incrassata* 1a genotypic cluster and sits on a long branch with 100% bootstrap support.

In most cases, our genotypic cluster species are monophyletic and can also be regarded genealogical species (Baum and Donoghue 1995). Interfertility assays confirm that, at least for what the *H. monile–simulans–incrassata* 2 clade is concerned, the genotypic cluster, genealogical, and biological species concepts correspond (unpublished data). The phylogenetic pattern within *H. incrassata* 1 hinders the equation of our genotypic cluster species with genealogical species. If *H. incrassata* 1b is to be considered a species, *H. incrassata* 1a is left nonmonophyletic in the ITS1–5.8S–ITS2 tree and thus does not comply with the genealogical species definition (Baum and Donoghue 1995). The interesting point is that the ITS1–5.8S–ITS2 tree shows a fundamental flaw of the genealogical species concept, namely that species may originate from other species and that, as a consequence hereof, monophyly does not always lead to a workable species definition. It cannot be judged from our data that both clusters within *H. incrassata* 1 comply with the biological species

TABLE 5. Key to species *Halimeda* of section *Rhipsalis*.

| | |
|---|---|
| 1 a | Segment surface rugose, appearing pitted. Peripheral utricles exceeding 110 μm in surface diameter and 170 μm in height . . . *H. favulosa* |
| 1 b | Segment surface smooth to somewhat rugose, very rarely appearing pitted. Peripheral utricles smaller . . . 2 |
| 2 a | Thallus with extensive (no less than 2 cm, often more than 4 cm high) basal zone made up of massive, stipitate, cylindrical to slightly flattened segments . . . 3 |
| 2 b | Basal zone different . . . 7 |
| 3 a | Cylindrical segments restricted to basal zone. Segments higher up the thallus flattened and broader than long. Peripheral utricles exceeding 40 μm in surface diameter and 45 μm in height . . . 4 |
| 3 b | Majority of segments higher up the thallus also cylindrical, never broader than high. Peripheral utricles smaller . . . *H. cylindracea* |
| 4 a | Supranodal siphons longer than 350 μm . . . 5 |
| 4 b | Supranodal siphons shorter . . . 6 |
| 5 a | Segment length exceeding 8.5 mm. Nodal fusions obvious; height of nodal fusions (including cell walls) exceeding 42 μm. Diameter of supranodal siphons exceeding 140 μm. Peripheral utricles exceeding 42% of their maximal width at 1/4th from their base. Subperipheral utricles markedly swollen, almost round *H. incrassata* 1b |
| 5 b | Segment length less than 8.5 mm. Nodal fusions not always obvious; height of nodal fusions not exceeding 42 μm. Diameter of supranodal siphons generally less than 140 μm. Peripheral utricles not generally reaching 42% of their maximal width at 1/4th from their base. Subperipheral utricles not markedly swollen, elongate . . . *H. incrassata* 1a |
| 6 a | The result of $[-3.4 \cdot (\text{width of peripheral utricles}) + 283\ \mu m]$ exceeds the height of the peripheral utricles. Nodal fusions always obvious; fusion height (including cell walls) exceeding 32 μm. Holdfast generally bulbous . . . *H. incrassata* 2 |
| 6 b | The result of the equation is less than the height of the peripheral utricles. Nodal fusions not always obvious; fusion height less than 38 μm. Holdfast generally matted . . . *H. incrassata* 1a |
| 7 a | Segment width exceeding 12.5 mm . . . *H. macroloba* |
| 7 b | Segment width smaller than 12.5 mm . . . 8 |
| 8 a | Peripheral utricles exceeding 56 μm in width and 72 μm in height . . . 6 |
| 8 b | Peripheral utricles smaller . . . 9 |
| 9 a | Width of peripheral utricles exceeding the result of $[-1.67 \cdot (\text{width of secondary utricles}) + 124\ \mu m]$ . . . 10 |
| 9 b | Width of peripheral utricles smaller than the result of the equation . . . 11 |
| 10 a | Nodal fusions obvious; height of nodal fusion (including cell walls) exceeding 30 μm. Length of supranodal siphon not exceeding 335 μm. Width of secondary utricles exceeding 42 μm . . . *H. incrassata* 2 |
| 10 b | Nodal fusions not always obvious; height of nodal fusion less than 30 μm. Length of supranodal siphon exceeding 335 μm. Width of secondary utricles smaller than 45 μm . . . *H. melanesica* |
| 11 a | Height over width ratio of peripheral utricles exceeding 1.6 . . . 12 |
| 11 b | Height over width ratio of peripheral utricles not exceeding 1.6 . . . 13 |
| 12 a | Length of supranodal siphons exceeding 300 μm. Height of nodal fusions (including cell walls) exceeding 45 μm. Width of peripheral utricles exceeding 30 μm . . . *H. monile* |
| 12 b | Supranodal siphons shorter than 300 μm. Height of nodal fusions less than 45 μm. Width of peripheral utricles less than 35 μm . . . *H. stuposa* |
| 13 a | Numerous cylindrical segments; longer than broad. Segment width smaller than the result of $[10.83 \cdot (\text{segment thickness}) - 15.33]$ . . . *H. monile* |
| 13 b | Segments rarely cylindrical; of variable shape, often about as broad as long or broader than long. Segment width bigger than the result of the equation . . . 14 |
| 14 a | Peripheral utricles exceeding 55 μm in height and 40 μm in width. Segment length over width ratio exceeding 0.9. Segment width less than 5.7 mm. Segment thickness less than 1 mm . . . 15 |
| 14 b | Peripheral utricles less than 55 μm in height, rarely exceeding 40 μm in width. Segment length over width ratio less than 0.9. Segment width exceeding 5.7 mm. Segment thickness exceeding 0.8 mm . . . 16 |
| 15 a | Attached to rocky substrate by means of a felty holdfast disc. Segment length over width ratio exceeding 0.9. Segment width less than 6 mm. Peripheral utricles reaching less than 45% of their maximal width at 1/4 of their height . . . *H. melanesica* |
| 15 a | Anchored in sand by means of a bulbous holdfast composed of rhizoids with attached grains of sand or anchored in silt by means of a long, slender tuft of rizoids. Segment length over width ratio usually less than 0.9. Segments generally broader than 6 mm. Peripheral utricles usually exceeding 45% of their maximal width at 1/4 of their height . . . *H. borneensis* |
| 16 a | Height of peripheral utricles exceeding the result of $[3 \cdot (\text{diameter of medullar siphons}) - 145]$ . . . *H. borneensis* |
| 16 b | Height of peripheral utricles smaller than the result of the equation . . . *H. simulans* |

Q1

The correctness of identifications based on this key is expected to decrease if segment selection and measurements do not follow the following guidelines. Juvenile specimens must be avoided. Ten segments must be chosen at random from the central region of the specimen (Verbruggen et al. 2005b). All segment measurements must be expressed in mm, and the median values over the 10 segments must be used in the key. One segment from the central region must be dissected according to Verbruggen et al. (2005a) and guidelines in this study. Anatomical measurements must be taken in 10-fold (see Materials and Methods) and expressed in μm. The median values of these 10 measurements must be used in the key. If these directions are not strictly followed, the use of the presented key is fundamentally faulty.

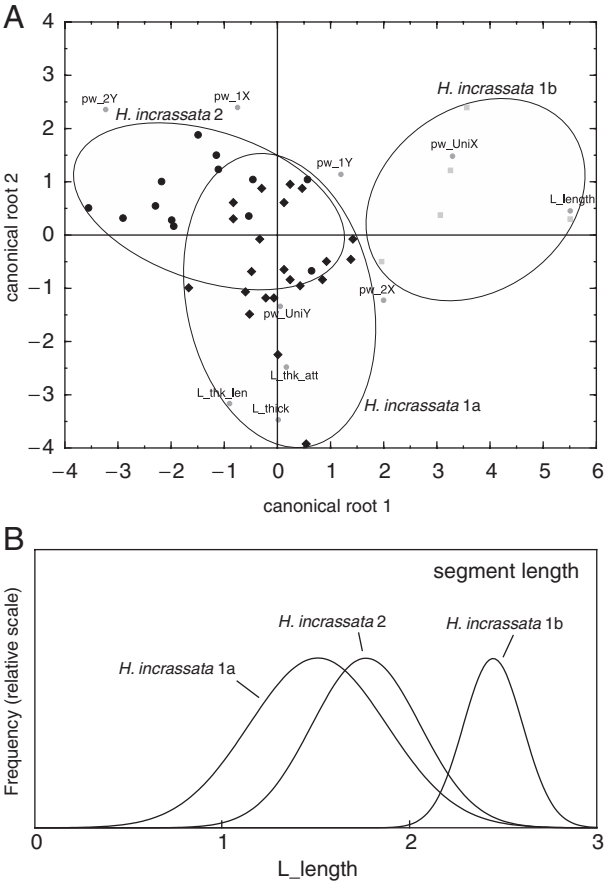


FIG. 6. Discrimination between *Halimeda incrassata* entities using segment morphological variables. (A) Canonical biplot of DA with variables s7, s11–s19 (log-transformed when necessary). (B) Estimated distribution of viariable L_length for the three *H. incrassata* entities. All based on data set of median values. Symbols as in Figures 4 and 5.

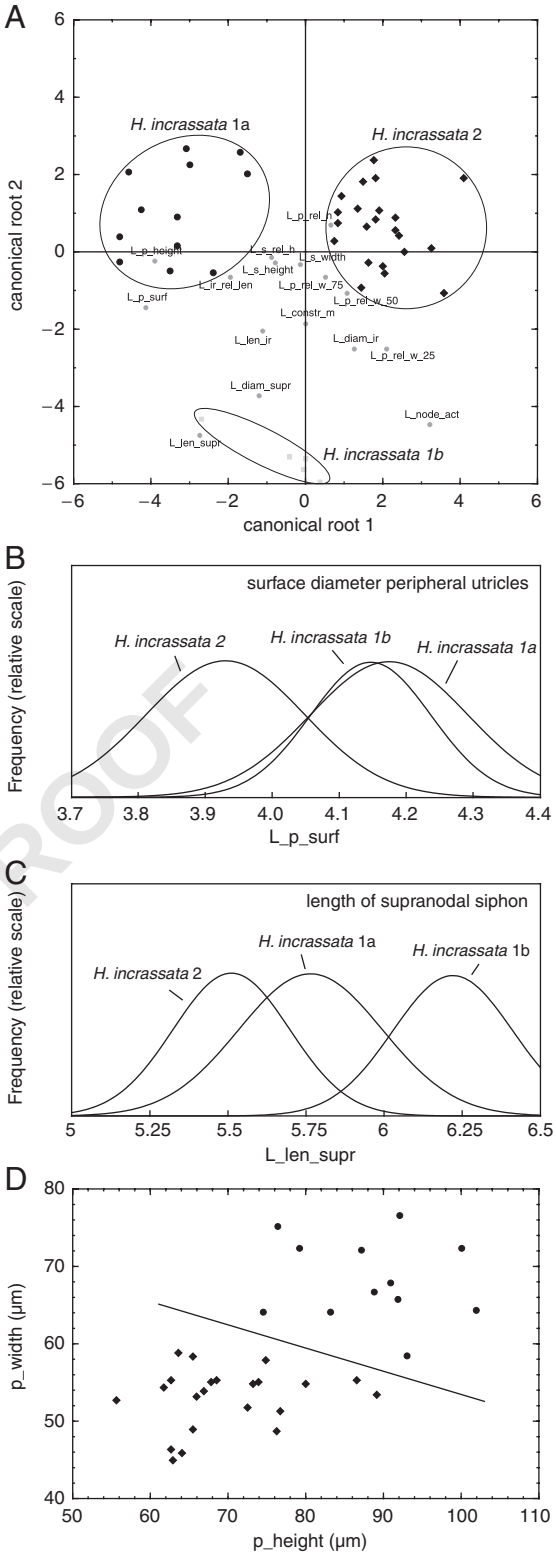


FIG. 7. Discrimination between *Halimeda incrassata* entities using anatomical variables. (A) Canonical biplot of DA with (log-transformed) variables a1–a12, a14–a20. (B) Estimated distribution of variable L_p_surf for the three *H. incrassata* entities. (C) Estimated distribution of variable L_len_supr for the three entities. (D) *Halimeda incrassata* 1a and 2 observations separate perfectly using two variables associated with peripheral utricles. All based on data set of median values.

concept. In any case, the problem is merely one of species definitions and does not hinder taxonomic inference from our morphometric data. Following the genotypic cluster species concept, *H. incrassata* 1a and 1b have been retained as different species in our analyses.

The topological discordance between the *rps*3 and ITS–5.8S–ITS2 trees is also of interest. The fact that *H. incrassata* 1b is recovered within *H. incrassata* 1a in one tree and as the closest sister of the *H. macroloba–incrassata* 1a clade in the other tree could indicate reticulate speciation or incomplete lineage sorting (Avise 2000). Our data do not allow identification of the discordance's cause. Verbruggen et al. (submitted) found multiple topological discordances in *Halimeda* section *Halimeda*, and we refer to their study for a more elaborate discussion of putative reticulate evolution within the genus *Halimeda*.

*Morphometrics*. The identification problems listed in the introduction are clearly reflected in PCA. Species in which identification problems are present or within which cryptic diversity is contained show partial to complete overlap in the biplots of all major principal

components. This is particularly obvious in the anatomical biplot, where the data are polarized into two major species groups, each of which contains a set of taxonomic problems. Given that the biplots represent the most obvious differences in the data, and thus reflect the absence of obvious differences between problem species, one should not be surprised that the section under study has suffered from misidentifications and taxonomic conservatism in the past.

The initial DAs shed light on the nature of similarities and differences between species. In the canonical biplot based on segment morphological characters, problematic species pairs occupy overlapping areas. Clear-cut separation of a few species in the first and second dimension of the canonical biplot based on anatomy indicates that anatomical characters hold more conclusive differences. This is confirmed by the much higher classification success of DA based on anatomical characters.

Separation of species using the data set of median values is much more complete than with the data set of 10 replicates per specimen, both for segment morphological and anatomical data. This is not surprising: By using medians, only the most representative values are retained and the edges of the variable distributions are considerably narrowed, accentuating interspecific differences and downplaying intraindividual morphological plasticity.

The conclusion of the explorative DA must be that morphological differences between species exist. From the significance of interspecific Mahalanobis distances and the success of classification tests, it can be concluded that these differences are highly significant. That DA points to significant differences between species does not imply that these differences correspond to those traditionally used in literature. It may even be that the differences are so mathematically complex that they cannot be translated into simple morphological clues for future identifications.

The issue of future identification of specimens has been approached in two ways. First, classification functions of DA offer a framework for probabilistic species identification. Second, interpretation of additional DA on increasingly trimmed-down data sets leads to an identification key. Before discussing these identification methods in more detail, a few taxonomic issues that could escape notice in the mathematical approach are stressed.

*Taxonomic remarks.* The principal character setting *H. melanesica* apart from species in section *Rhipsalis* is the absence of nodal fusions and the matted holdfast in the former (Valet 1966, Hillis-Colinvaux 1980). With the discovery of small nodal fusions in *H. melanesica*, Noble (1987) stressed the blurring of the boundary between *H. melanesica* and *H. incrassata*. The present study sheds more light on the identity of and distinction between *H. melanesica* and the different *H. incrassata* species. Whereas the species *H. incrassata* 1b and 2 contain specimens with large nodal fusions, the genotypic clusters given the denomination *H. melanesica* and *H. incrassata* 1a contain specimens without and with minute nodal pores. The genotypic clusters with specimens featuring small nodal pores were given their names on the basis of the presence of a matted holdfast in all specimens with a *H. melanesica* DNA bar code and the presence of a more extensive holdfast in certain specimens bearing a *H. incrassata* 1a bar code. External morphological characters do not allow unequivocal designation of specimens to *H. incrassata* 1a or *H. melanesica*, but the distinction can easily be made on the basis of anatomical measurements. The most obvious difference is the size of peripheral utricles. Medians of surface diameter and height do not exceed 50 μm and 67 μm, respectively, in *H. melanesica*. Peripheral utricles of our specimens of *H. incrassata* 1a are larger: no less than 57 μm in diameter and 74 μm in height. Post-hoc morphometric examination of the type specimen of *H. melanesica* (PC0021851, Muséum National d'Histoire Naturelle, Paris [PC]) confirms that the genotypic cluster given the *H. melanesica* denomination is indeed *H. melanesica*. Morphological distinction between the three *H. incrassata* genotypic cluster species is less straightforward. Especially clusters 1a and 2 are difficult to discern between using morphometric data. For details on the distinguishing characters, we refer to lines four to six of the identification key (Table 5).

Information on the origin of specimens can help in their identification. In our definition, *H. borneensis* seems to be restricted to the Indo-Pacific and *H. simulans* to the Atlantic. Even though certain specimens belonging to the *H. borneensis* genotypic cluster were identified as *H. simulans* on the basis of a previous monograph (Hillis-Colinvaux 1980), no specimens belonging to the *H. simulans* genotypic cluster were found in the Indo-Pacific. Based on this finding, it seems likely that all Indo-Pacific records of *H. simulans* are false and to be considered *H. borneensis*. Similarly, *H. incrassata* 1a and *H. cylindracea* are restricted to the Indo-Pacific, whereas *H. incrassata* 2 and *H. monile* occur only in the Atlantic. In the light of our results, reports of *H. monile* in Indo-Pacific waters should be considered erroneous until their identity is reconfirmed using DNA bar coding or the identification methods presented here. Despite the fact that geographic information seems very useful for identification of certain *Halimeda* species, it should be used with extreme caution because seaweeds are among the most prevalent invasive marine species (Jousson et al. 2000, Rueness and Rueness 2000, De Clerck et al. 2002). *Halimeda opuntia*, a profuse pantropical species, is believed to have invaded in the Caribbean during the last millennium (Kooistra and Verbruggen 2005).

*Probabilistic identification approach.* Identification of specimens comes down to allocating them to groups at the specific rank in a taxonomic framework. Inferring the species to which a specimen belongs is a matter of following identification rules prescribed by systematists. In biological taxonomy, it usually concerns morphological identification rules, and

systematists tend to compact such rules into dichotomous identification keys that lead to unambiguous (absolute) allocation of specimens to species.

There are, however, alternative ways to approach identification. On the one hand, the kind of data can be altered (e.g. physiological properties, DNA bar codes). On the other hand, the identification rules can be probabilistic rather than absolute. This means that following the identification rules leads to probability values for each species considered. In essence, absolute identification is a mere variant of probabilistic identification with the probabilities for all but one species equal to 0 and the probability of one species equal to 1. Probabilistic methods are most often used if the characters used do not allow absolute identification or when large amounts of information have to be processed automatically (e.g. in clinical microbiology [Gyllenberg and Koski 2002, Kassama et al. 2002]).

We provide a probabilistic method of specimen identification on the basis of anatomical measurements for species of *Halimeda* section *Rhipsalis* (Table 4). If measurements on new specimens are taken according to the methods described in this study and in Verbruggen et al. (2005a,b), the classification functions can be used to calculate scores for each of the 10 species included in our morphometric analyses. The species obtaining the highest score is the taxon to which the specimen belongs with the highest probability.

*Identification key construction*. For the construction of an identification key, further DAs were carried out on trimmed-down data sets. The identification key incorporates traditional as well as morphometric data and leads to 100% correct identifications for the specimens incorporated in this study.

The DAs expose the importance of characters for species differentiation. Segment morphological characters do not usually allow for delineation of species or groups of species. This does not mean that segment characteristics do not contain any useful information but that on the basis of segment data alone, one cannot make the distinction between all species. Anatomical data provide much better diagnostic characters, validating the results of Verbruggen et al. (2005a) and further stressing that the trend of increasing focus on anatomy for identification purposes continues. Anatomy is the key to discern between cryptic entities and look-alikes. Therefore, identification based on superficial comparison is firmly discouraged.

Not all anatomical characters are equally important for species recognition. Especially peripheral utricles yield taxonomically useful measurements, substantiating the attention paid to these measurements by former systematists. Nonetheless, certain measurements not or rarely used in previous taxonomic treatises prove useful in a number of cases. Examples are nodal fusion height (a08), the distance between the nodal fusion and the first ramification of the siphon above the node (a09), and diameter of medullar siphons (a01).

It is difficult to predict whether and how addition of specimens to our data set will influence the correctness of the identification key. We have strived for representative sets of specimens of the different species, not avoiding specimens in the gray zone between morpho-species. Certain species were included merely to sketch a more complete picture even though they can easily be recognized using classical characters (e.g. *H. macroloba*). On the other hand, certain species are underrepresented in our data because they are rare or highly geographically restricted (e.g. *H. melanesica*, *H. stuposa*). Whether or not the threshold values used in the identification keys need to be updated when increasing numbers of specimens are added remains an open question.

We are appreciative to the Bijzonder Onderzoeksfonds (Ghent University, grant 011D9101), the Fund for Scientific Research Flanders (grant 3G002496 and postdoctoral fellowship to O. D. C.), and the Leopold III Fund. We thank E. Cocquyt for her assistance with the molecular work. C. De maire and C. VanKerckhove are acknowledged for caring over the GENT herbarium collection and database and for assistance with administration. We thank K. Page, H. Spalding, and P. Vroom for providing us with the Hawaiian *H. incrassata* specimens and L. de Senerpont-Domis and W. Prud'homme van Reine for a collection of Indonesian material. We thank K. Arano, M. A. Coffroth, P. Colinvaux, O. Dargent, G. De Smedt, F. Gurgel, O. A. Gussmann, I. Hendriks, L. Hillis, F. Leliaert, L. Liao, C. Payri, W. Prud'homme van Reine, M. van Veghel, B. Wysor, F. Zechman, and G. Zuccarello for various collections. M. Wynne is acknowledged for sending the type material of *H. borneensis*. H. V. acknowledges Claude Payri, Paino Vanai, and the Environmental Service of Wallis and Futuna for facilitating fieldwork on Uvea Island. H. V. further thanks T. and C. Leigh, D. Olandesca, R. Diaz, and C. Galanza for their helping hands during expeditions. Two anonymous reviewers are acknowledged for their constructive remarks.

Avise, J. C. 2000. *Phylogeography. The History and Formation of Species*. Harvard University Press, Cambridge, MA, 447 pp.

Barton, E. S. 1901. *The Genus Halimeda. Monographs of the Siboga Expedition*. Vol. 60. Leiden, The Netherlands, 32 pp.

Baum, D. A. & Donoghue, M. J. 1995. Choosing among alternative phylogenetic species concepts. *Syst. Bot.* 20:560–73.

Besansky, N. J., Severson, D. W. & Ferdig, M. T. 2003. DNA barcoding of parasites and invertebrate disease vectors: what you don't know can hurt you. *Trends Parasitol.* 19:545–6.

Cohen, S., Faugeron, S., Martinez, E. A., Correa, J. A., Viard, F., Destombe, C. & Valero, M. 2004. Molecular identification of two sibling species under the name *Gracilaria chilensis* (Rhodophyta, Gracilariales). *J. Phycol.* 40:742–7.

De Clerck, O., Anderson, R. J., Bolton, J. J. & Robertson-Andersson, D. 2002. *Schimmelmannia elegans* (Gloiosiphoniaceae, Rhodophyta): South Africa's first introduced seaweed? *Phycologia* 41:184–90.

Felsenstein, J. 1985. Confidence limits on phylogenies: an approach using the bootstrap. *Evolution* 39:783–91.

Gurgel, C. F. D., Liao, L. M., Fredericq, S. & Hommersand, M. H. 2003. Systematics of *Gracilariopsis* (Gracilariales, Rhodophyta) based on *rbc*L sequence analyses and morphological evidence. *J. Phycol.* 39:154–71.

Gyllenberg, M. & Koski, T. 2002. Bayesian predictiveness, exchangeability and sufficientness in bacterial taxonomy. *Math. Biosci.* 177:161–84.

Hebert, P. D. N., Penton, E. H., Burns, J. M., Janzen, D. H. & Hallwachs, W. 2004a. Ten species in one: DNA barcoding reveals cryptic species in the neotropical skipper butterfly *Astraptes fulgerator*. *Proc. Natl. Acad. Sci. USA* 101:14812–7.

Hebert, P. D. N., Stoeckle, M. Y., Zemlak, T. S. & Francis, C. M. 2004b. Identification of birds through DNA barcodes. *PLoS Biol.* 2:e312.

Hillis-Colinvaux, L. 1980. Ecology and taxonomy of *Halimeda*: primary producer of coral reefs. *Adv. Mar. Biol.* 17:1–327.

Hogg, I. D. & Hebert, P. D. N. 2004. Biological identification of springtails (Hexapoda: Collembola) from the Canadian Arctic, using mitochondrial DNA barcodes. *Can. J. Zool.* 82:749–54.

Jousson, O., Pawlowski, J., Zaninetti, L., Zechman, F. W., Dini, F., Di Guiseppe, G., Woodfield, R., Millar, A. & Meinesz, A. 2000. Invasive alga reaches California. *Nature* 408:157–8.

Kassama, Y., Rooney, P. J. & Goodacre, R. 2002. Fluorescent amplified fragment length polymorphism probabilistic database for identification of bacterial isolates from urinary tract infections. *J. Clin. Microbiol.* 40:2795–800.

Kooistra, W. H. C. F., Coppejans, E. G. G. & Payri, C. 2002. Molecular systematics, historical ecology, and phylogeography of *Halimeda* (Bryopsidales). *Mol. Phylogenet. Evol.* 24:121–38.

Kooistra, W. H. C. F. & Verbruggen, H. 2005. Genetic patterns in the calcified tropical seaweeds *Halimeda opuntia*, *H. distorta*, *H. hederacea* and *H. minima* (Bryopsidales, Chlorophyta) provide insights in species boundaries and inter-oceanic dispersal. *J. Phycol.*, (in press).

Knowlton, N. 1993. Sibling species in the sea. *Annu. Rev. Ecol. Syst.* 24:189–216.

Lamouroux, J. V. F. 1812. Extrait d'un mémoire sur la classification de polypes coralligènes non entièrement pierreux. *Nouv. Bull. Sci. Soc. Philomath.* 3:181–8.

Noble, J. M. 1987. *A Taxonomic Study of the Genus* Halimeda *Lamouroux (Chlorophyta, Caulerpales) From the Heron Island Region of the Southern Great Barrier Reef, Australia*. Masters degree thesis, University of Melbourne, Melbourne, Australia, 200 pp.

Provan, J., Murphy, S. & Maggs, C. A. 2004. Universal plastid primers for Chlorophyta and Rhodophyta. *Eur. J. Phycol.* 39:43–50.

Rohlf, F. J. 2004. *tpsDig version 1.40*. Department of Ecology and Evolution, State University of New York at Stony Brook. Available for download from http://life.bio.sunysb.edu/morph/

Rueness, J. & Rueness, E. 2000. *Caulacanthus ustulatus*. (Gigartinales, Rhodophyta) from Brittany (France) is an introduction from the Pacific Ocean. *Cryptog. Algol.* 21:355–63.

Swofford, D. L. 2003. *Paup*. Phylogenetic Analysis Using Parsimony (*And Other Methods)*. Version 4. Sinauer Associates, Sunderland, MA.

Valet, G. 1966. Sur une espèce rare et une nouvelle espèce d'*Halimeda* de Mélanésie. *Rev. Gén. Botan.* 73:680–5.

van der Strate, H. J., Boele-Bos, S. A., Olsen, J. L., van de Zande, L. & Stam, W. T. 2002. Phylogeographic studies in the tropical seaweed *Cladophoropsis membranacea* (Chlorophyta, Ulvophyceae) reveal a cryptic species complex. *J. Phycol.* 38:572–82.

Verbruggen, H., De Clerck, O., Cocquyt, E., Kooistra, W. H. C. F. & Coppejans, E. 2005a. Morphometric taxonomy of siphonous green algae: a methodological study within the genus *Halimeda* (Bryopsidales). *J. Phycol.*, (in press).

Verbruggen, H., De Clerck, O. & Coppejans, E. 2005b. Deviant segments hamper a morphometric approach towards *Halimeda* taxonomy. *Cryptog. Algol.*, (in press).

Verbruggen, H., De Clerck, O., Schils, T., Kooistra, W. H. C. F. & Coppejans, E. Evolution and phylogeography of the *Halimeda cuneata/discoidea/tuna* cryptic species complex.

Verbruggen, H. & Kooistra, W. H. C. F. 2004. Morphological characterization of lineages within the calcified tropical seaweed genus *Halimeda* (Bryopsidales, Chlorophyta). *Eur. J. Phycol.* 39:213–28.

Yano, T., Kamiya, M., Arai, S. & Kawai, H 2004. Morphological homoplasy in Japanese *Plocamium* species (Plocamiales, Rhodophyta) inferred from the Rubisco spacer sequence and intracellular acidity. *Phycologia* 43:383–93.

Zuccarello, G. C. & West, J. A. 2002. Phylogeography of the *Bostrychia calliptera–B. pinnata* complex (Rhodomelaceae, Rhodophyta) and divergence rates based on nuclear, mitochondrial and plastid DNA markers. *Phycologia* 41:49–60.

Zuccarello, G. C. & West, J. A. 2003. Multiple cryptic species: molecular diversity and reproductive isolation in the *Bostrychia radicans/B. moritziana* complex (Rhodomelaceae, Rhodophyta) with focus on North American isolates. *J. Phycol.* 39:948–59.

Q6 Q6 Q6 Q1

Appendix 1. Specimen list

| Species | Specimen | Geographical origin | ITS | *rps*3 | Segment | Anatomy |
|---|---|---|---|---|---|---|
| *Halimeda borneensis* | 10101E | Maisel Islands, Indonesia | AF525558 | | | |
| | cc38608 (MICH) | Borneo, Indonesia (holotype) | | | + | |
| | H.0042 | Moorea, French Polynesia | AF525552 | | | |
| | H.0043 | Moorea, French Polynesia | AF525553 | | | |
| | H.0044 | Moorea, French Polynesia | AF525554 | | | |
| | H.0170 | Pangasinan, The Philippines | AF525557 | | | |
| | H.0174 | Pangasinan, The Philippines | AF525555 | | | |
| | H.0267 | New Caledonia | AF525550 | | | |
| | H.0269 | New Caledonia | AF525551 | | | |
| | HEC12603a | Chwaka, Zanzibar, Tanzania | AF407239 | | | |
| | HEC12603b | Chwaka, Zanzibar, Tanzania | AF525559 | | | |
| | HV18-1 | Chwaka, Zanzibar, Tanzania | AY786512 | AY835514 | + | + |
| | HV23c | Chwaka, Zanzibar, Tanzania | | | + | + |
| | HV92 | Moorea, French Polynesia | AY835458 | AY835515 | + | + |
| | HV145 | Moorea, French Polynesia | | AY835516 | + | + |
| | HV183a | Arue, Tahiti, French Polynesia | AY835459 | AY835517 | + | + |
| | HV183b | Arue, Tahiti, French Polynesia | AY786513 | AY835518 | + | + |
| | HV205 | Faaa, Tahiti, French Polynesia | AY835460 | AY835519 | + | + |
| | HV208 | Faaa, Tahiti, French Polynesia | | AY835520 | + | + |
| | HV245 | Maraa, Tahiti, French Polynesia | AY835461 | AY835521 | + | + |
| | HV246 | Maraa, Tahiti, French Polynesia | AY835462 | AY835522 | + | + |
| | HV639 | Olango, The Philippines | AY835463 | AY835523 | + | + |
| | HV733 | Uson, The Philippines | AY835464 | AY835524 | + | + |
| | PH534 | Zamboanga, The Philippines | | AY835525 | + | + |
| | WLS081-02 | Wallis Island (Pacific Ocean) | | AY835526 | + | + |
| | WLS086-02 | Wallis Island (Pacific Ocean) | AY835465 | AY835527 | + | + |
| | WLS148-02 | Wallis Island (Pacific Ocean) | AY835466 | AY835528 | + | + |
| | | Zamboanga, The Philippines | AF525556 | | | |
| *H. cylindracea* | H.0015 | Great Barrier Reef, Australia | AF525549 | | + | + |

APPENDIX 1 (Continued)

| Species | Specimen | Geographical origin | ITS | *rps*3 | Segment | Anatomy |
|---|---|---|---|---|---|---|
| | H.0018 | Great Barrier Reef, Australia | AF525548 | | | |
| | H.0186 | Great Barrier Reef, Australia | AF416388 | | | |
| | H.0279 | New Caledonia | AF407236 | | | |
| | HOD-PH99-4 | Bantayan, The Philippines | AY835467 | | + | + |
| | SOC364 | Socotra (Yemen) | AF525546 | | | |
| | | Great Barrier Reef, Australia | AF525545 | | | |
| *H. incrassata* 1a | 03-104 (L) | Panjang, Indonesia | AY835468 | | + | + |
| | H.0016 | Great Barrier Reef, Australia | AY835469 | AY835529 | + | + |
| | H.0019 | Great Barrier Reef, Australia | AF525572 | AY835530 | + | + |
| | H.0022 | Great Barrier Reef, Australia | AF525571 | | | |
| | H.0035 | Tahiti, French Polynesia | AF407242 | | | |
| | H.0036 | Tahiti, French Polynesia | AF525569 | | | |
| | H.0040 | Rangiroa, French Polynesia | AF525570 | | | |
| | H.0045 | Rangiroa, French Polynesia | AF525573 | | | |
| | HV22 | Chwaka, Zanzibar, Tanzania | | AY835531 | + | + |
| | HV104 | Moorea, French Polynesia | AY835470 | AY835532 | + | + |
| | HV144 | Moorea, French Polynesia | AY835471 | AY835533 | + | + |
| | HV146 | Moorea, French Polynesia | | AY835534 | + | + |
| | HV149 | Moorea, French Polynesia | AY835472 | AY835535 | + | + |
| | HV231 | Maraa, Tahiti, French Polynesia | | AY835536 | + | + |
| | HV629 | Olango, The Philippines | AY835473 | AY835537 | + | + |
| | HV636 | Olango, The Philippines | AY835474 | AY835538 | + | + |
| | HV763 | Tangat, The Philippines | AY835475 | AY835539 | + | + |
| | PH197 | Mactan, The Philippines | AF407241 | | + | |
| | | Mactan, The Philippines | AF525568 | | | |
| *H. incrassata* 1b | H.0649 | Honolua Bay, Maui, Hawaii, USA | AY835476 | AY835540 | + | + |
| | H.0650 | Honolua Bay, Maui, Hawaii, USA | AY835477 | AY835541 | + | + |
| | H.0651 | Honolua Bay, Maui, Hawaii, USA | AY835478 | AY835542 | + | + |
| | H.0652 | Honolua Bay, Maui, Hawaii, USA | AY835479 | AY835543 | + | + |
| | H.0653 | Honolua Bay, Maui, Hawaii, USA | AY835480 | | + | + |
| *H. incrassata* 2 | H.0027 | Galeta, Panama | | AY835544 | + | + |
| | H.0077 | Bocas del Toro, Panama | AY835481 | AY835545 | + | + |
| | H.0079 | Bocas del Toro, Panama | AY835482 | AY835546 | + | + |
| | H.0127 | Bocas del Toro, Panama | AY835483 | AY835547 | + | + |
| | H.0132 | San Andres, Panama | AY835484 | AY835548 | + | + |
| | H.0136 | St. Martin, Netherlands Antilles | AY835485 | AY835549 | + | + |
| | H.0143 | Isla Grande, Panama | AY835486 | AY835550 | + | + |
| | H.0145 | Florida, USA | | | + | + |
| | H.0146 | Florida, USA | | | + | + |
| | H.0149 | Florida, USA | AY835487 | AY835551 | + | + |
| | H.0179 | Lee Stocking, Bahamas | AF407233 | AY835552 | + | + |
| | H.0180 | Florida, USA | AY835488 | AY835553 | + | + |
| | H.0181 | Florida, USA | AF525537 | AY835554 | + | + |
| | H.0182 | Florida, USA | | AY835555 | + | + |
| | H.0183 | Florida, USA | AF525538 | AY835556 | + | + |
| | H.0188 | Bocas del Toro, Panama | AY835489 | AY835557 | + | + |
| | H.0211 | San Blas, Panama | AF525539 | | | |
| | H.0229 | Puerto Morelos, Mexico | AY835490 | AY835558 | + | + |
| | H.0236 | Texas, USA | AF525540 | | | |
| | H.0248 | San Blas, Panama | | AY835559 | + | + |
| | H.0477 | Bocas del Toro, Panama | | AY835560 | + | + |
| | HV332 | St. Ann's Bay, Jamaica | AY835491 | AY835561 | + | + |
| | HV334 | St. Ann's Bay, Jamaica | AY835492 | | + | + |
| | HV448 | Discovery Bay, Jamaica | AY835493 | | + | + |
| *H. macroloba* | H.0038 | Tahiti, French Polynesia | AF525563 | | | |
| | H.0060 | Viti Levu, Fiji | AF525564 | | | |
| | H.0157 | Pangasinan, The Philippines | AF525560 | | | |
| | H.0158 | Pangasinan, The Philippines | AF525566 | | | |
| | H.0228 | Exmouth, W Australia | AF525562 | | | |
| | HEC12583 | Zanzibar, Tanzania | AF407240 | | | |
| | HV5 | Matemwe, Zanzibar, Tanzania | | | + | |
| | HV17 | Chwaka, Zanzibar, Tanzania | | | + | |
| | HV38 | Nungwi, Zanzibar, Tanzania | AY786514 | AY835562 | + | + |
| | HV206 | Faaa, Tahiti, French Polynesia | AY786515 | | + | + |
| | | Zanzibar, Tanzania | AF525561 | | | |
| | | Zamboanga, The Philippines | AF525565 | | | |
| | | Great Barrier Reef, Australia | AF525567 | | | |
| *H. melanesica* | 03-462 (L) | Maratua, Indonesia | AY835494 | AY835563 | + | + |
| | HV217 | Afaahiti, Tahiti, French Polynesia | AY835495 | AY835564 | + | + |
| | HV790 | Bulusan, Luzon, The Philippines | AY835496 | AY835565 | + | + |

APPENDIX 1 (Continued)

| Species | Specimen | Geographical origin | ITS | *rps*3 | Segment | Anatomy |
|---|---|---|---|---|---|---|
| | HV818 | Dancalan, Luzon, The Philippines | AY835497 | AY835566 | + | + |
| *H. monile* | H.0034 | Galeta, Panama | AY835498 | | + | + |
| | H.0075 | Bocas del Toro, Panama | AY835499 | | + | + |
| | H.0135 | San Andres, Panama | AY835500 | AY835567 | + | + |
| | H.0137 | St. Martin, Netherlands Antilles | AY835501 | AY835568 | + | + |
| | H.0228b | Puerto Morelos, Mexico | AF407234 | AY835569 | + | + |
| | H.0404 | Isla Grande, Panama | AY835502 | | | |
| | HV333 | St. Ann's Bay, Jamaica | AY835503 | AY835570 | + | + |
| | HV335 | St. Ann's Bay, Jamaica | AY835504 | AY835571 | + | + |
| | HV344 | Drax Hall, Ocho Rios, Jamaica | AY835505 | AY835572 | + | + |
| *H. simulans* | H.0032 | Galeta, Panama | AY835506 | AY835573 | + | + |
| | H.0071 | Bocas del Toro, Panama | AY835507 | AY835574 | + | + |
| | H.0080 | Bocas del Toro, Panama | AY835508 | AY835575 | + | + |
| | H.0114 | Portobelo, Panama | | AY835576 | + | + |
| | H.0147 | Florida, USA | | AY835577 | + | + |
| | H.0230 | Puerto Morelos, Mexico | AF525541 | AY835578 | + | + |
| | H.0324 | San Blas, Panama | AF525544 | | | |
| | H.0367 | Escudo de Veraguas, Panama | AF407235 | | | |
| | H.0402 | Isla Grande, Panama | AY835509 | | | |
| | HOD-MAR01-43 | Martinique, French Antilles | | | + | + |
| | HV361 | Drax Hall, Ocho Rios, Jamaica | AY835510 | AY835579 | + | + |
| | HV449 | Discovery Bay, Jamaica | AY835511 | AY835580 | + | + |
| | HV504 | Ocho Rios, Jamaica | AY835512 | AY835581 | + | + |
| | HV532 | Blue Lagoon, Portland, Jamaica | AY835513 | AY835582 | + | + |
| | | Isla Providencia, Colombia | AF525542 | | | |
| | | Galeta, Panama | AF525543 | | | |
| *H. stuposa* | L.0238148 (L) | Rongelap, Marshall Islands (isotype) | | | + | + |
| | L.0238149 (L) | Eniwetok, Marshall Islands (isotype) | | | + | + |

Specimen numbers correspond to their accession numbers in the Ghent University Herbarium (GENT), unless other herbarium acronyms are indicated in brackets (L = NHN Leiden, MICH = University of Michigan Herbarium). The last four columns represent the GenBank accession numbers of ITS and *rps*3 sequences and inclusion in segment morphological and anatomical morphometric databases. Species authorities of all species cited in the text are *H. borneensis* W.R. Taylor, *H. cylindracea* Decaisne, *H. incrassata* (J. Ellis) J.V. Lamouroux, *H. macroloba* Decaisne, *H. melanesica* Valet, *H. monile* (J. Ellis & Solander) J.V. Lamouroux, *H. simulans* M.A. Howe, *H. stuposa* W.R. Taylor.

# Author Query Form

Journal **JPY**

Article **04216**

**1. Disk Usage :-**

☐ Disk not provided

☑ Disk used

☐ Disk not used

- ☐ Disk is corrupt
- ☐ Unknown file format
- ☐ Virus found

☐ Additional Work done:

**2. Queries :-**

While preparing this paper/manuscript for typesetting, the following queries have arisen.

| Query No. | Page No. | Description | Author Response |
|---|---|---|---|
| Q1 | 2 | AU: This ref must be accepted and at least "in press" to remain as a text cite. Update to add year if it is in press, or if it is not yet accepted, delete here (and in the ref list) and cite as "unpublished data." | |
| Q2 | 2 | AU: Provide url, website address, or reference | |
| Q3 | 6 | AU: Verify end number | |
| Q4 | 6 | AU: Figures are misnumbered -- verify figure numbers throughout as renumbered per legends | |
| Q5 | 13 | AUI: Provide publisher | |
| Q6 | 14 | AU: Update, if possible, changing year here and throughout text if necessary | |
| Q7 | 3 | AU: Provide 3 column heads for the 3 columns presented | |
| | | | |